

516-18

16-1392

7/17/98

AAS 98-362

Improved Instrumental Magnitude Prediction Expected from Version 2 of the NASA SKY2000 Master Star Catalog*

C.B.Sande†, D.Brasoveanu, A.C.Miller, A.T.Home, (Computer Sciences Corp.),
D.A.Tracewell (NASA/GSFC), W.H.Warren Jr. (Raytheon STX)

The *SKY2000 Master Star Catalog (MC), Version 2* and its predecessors have been designed to provide the basic astronomical input data needed for satellite acquisition and attitude determination on NASA spacecraft. Stellar positions and proper motions are the primary *MC* data required for operations support followed closely by the stellar brightness observed in various standard astronomical passbands. The instrumental red-magnitude prediction subsystem (REDMAG) in the MMSCAT software package computes the expected instrumental color index (CI) [sensor color correction] from an observed astronomical stellar magnitude in the *MC* and the characteristics of the stellar spectrum, astronomical passband, and sensor sensitivity curve. The computation is more error prone the greater the mismatch of the sensor sensitivity curve characteristics and those of the observed astronomical passbands. See Figure 3 for comparison of the sensitivity curve of a typical new-generation red-sensitive charge-coupled-device (CCD) star tracker (ST) with the standard passbands (*UBVRJ*). Here, the effective wavelength of the very broad sensor curve is shifted well away from that of the much narrower visual (*V*) passband.

This paper presents the preliminary performance analysis of a typical red-sensitive CCDST during acquisition of sensor data from the two Ball CT-601 ST's onboard the Rossi X-Ray Timing Explorer (RXTE). A comparison is made of relative star positions measured in the ST FOV coordinate system with the expected results computed from the recently released *Tycho Catalogue* (Reference 1). The comparison is repeated for a group of observed stars with nearby, bright neighbors in order to determine the tracker behavior in the presence of an interfering near neighbor (NN). The results of this analysis will be used to help define a new photoelectric photometric instrumental sensor magnitude system (*S*) that is based on several thousand bright star magnitudes observed with the RXTE ST's. This new system will be implemented in *Version 2* of the *SKY2000 MC* to provide improved predicted magnitudes in the mission run catalogs.

* This work was supported by the National Aeronautics and Space Administration (NASA)/Goddard Space Flight Center (GSFC), Greenbelt, Maryland, USA, under Contract GS-35F-4381G, Task Order No. S-03365-Y.

† e-mail: csande@cscmail.csc.com

INTRODUCTION

The current operational version of the *SKYMAP MC*, known as *SKY2000 MC, Version 1* was produced in 1996-7 and represents the last version of the *MC* to contain data solely from ground-based sources. It is to be replaced by *SKY2000 MC, Version 2*, which will incorporate data from several newly available spaceborne sources, including astrometric and photometric data from the European Space Agency (ESA) Hipparcos mission and sensor photometric data acquired from the RXTE spacecraft. This catalog is to be a comprehensive all-sky star catalog down to approximately visual magnitude 9 that includes astrometric, photometric, and many other types of stellar data for approximately 300,000 stars. The MMSCAT software package is used to generate specialized subcatalogs called mission run catalogs for satellite attitude support using the *SKY2000 MC, Version 2* as input. All mission run catalog stars include a predicted sensor magnitude (m_s) calculated by the REDMAG subsystem. The observed sensor magnitudes from the RXTE ST's will provide an additional group of input magnitudes to the software for several thousand of the brightest stars.

BACKGROUND

Rossi X-Ray Timing Explorer:

The RXTE spacecraft was launched by a Delta II ELV on December 30, 1995, to study the time variability in emissions of x-ray sources over the spectral range 2-250 keV. Two Ball CT-601 CCDST's were carried as part of the spacecraft's attitude control system (ACS). Each tracker is capable of identifying up to five stars simultaneously for use in attitude determination (see Figure 1). Beginning in March, 1997, the Attitude Model Support Task began collecting additional star observations from both star trackers to refine the sensor calibration, to define a new observed photometric sensor system (*S*) for the *MC, Version 2*, and to determine near neighbor (NN) effects on measured sensor positions and magnitudes. In less than six months, more than 7700 observations have been obtained of several thousand different stars. Sky coverage has not been uniform because of mission constraints, but enough sensor magnitudes have been obtained to allow the creation of a new observed RXTE photometric sensor system. Stars having observed RXTE magnitudes will have magnitudes available that will more nearly match the effective wavelength and bandwidth of other CCDST's than those observed in the standard *UBVRI* passbands. Predicted instrumental m_s 's based upon RXTE input magnitudes are expected to be improved over those based upon the *UBVRI* passbands. The data acquired permit an examination of CCDST performance, primarily in the areas of measured star positions and measured sensor magnitudes, which are the most important pieces of information coming out of the ST's from the operational standpoint. The knowledge gained will be of use in improving the generation of future mission run catalogs for other satellites using CCDST's.

XTE Spacecraft

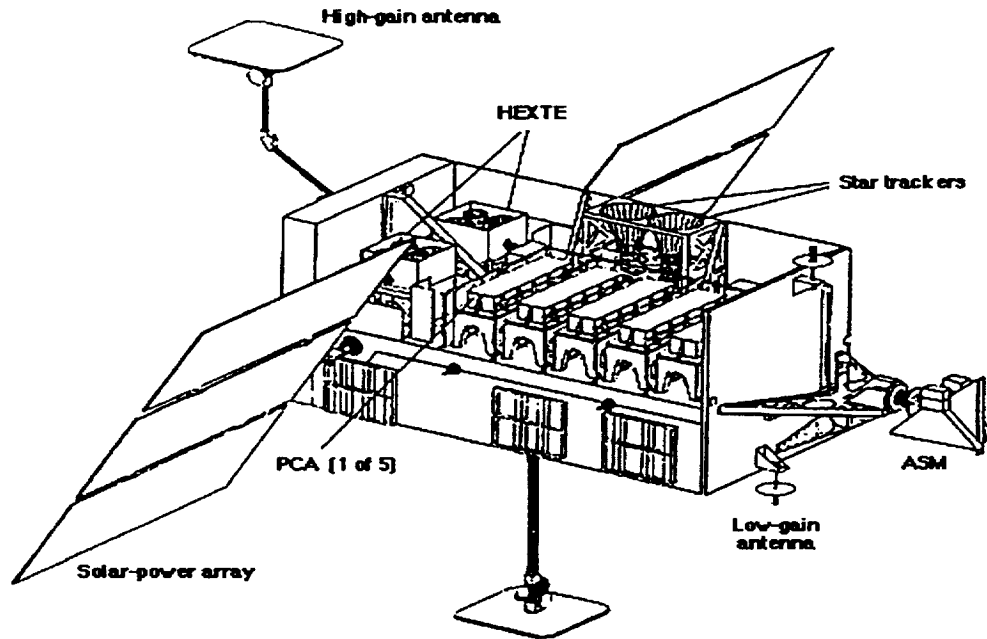


Figure 1 Rossi X-ray Timing Explorer

Characterization of the CCDST Data:

The body of data acquired by the Attitude Model Support Task includes measured positions in field of view (FOV) coordinates and measured instrumental magnitudes with data points at two-second intervals during periods of successful star identification. Observations were acquired both during periods of spacecraft inertial pointing and during slews between points. Up to five stars may be identified simultaneously by each star tracker. The trackers are mounted with a boresight separation of 9.9 degrees along the diagonal of each FOV, so that there is a little more than one degree in common between the nominal 8x8 degree FOV's at the overlapping corners. This arrangement allows for the possibility of simultaneous observation of the same star by both trackers.

Each star image detected by the CCDST is defocused so that its image is spread over 4x4 to 5x5 pixels. Each pixel on the CCD is approximately 60x60 arcsecond. The calculated centroid of this defocused image over 16 to 25 pixels yields a position in FOV coordinates and integration of the flux over the same image yields a sensor magnitude. Since a real-time spacecraft attitude was not recorded during the data acquisition, only the angular separation of neighboring pairs of stars in the FOV at the same time is useful in comparison with other independent source catalog positions (e.g., the *Tycho Catalogue* [Ref. 1]).

Stars which were mis-identified in the attitude determination software used to process the star tracker data were identified by the large deviations in the measured angular separation from that predicted for the

pair. These large deviations were typically on the order of several degrees and were well outside the range of variation examined for NN effects.

A comparison of the observed RXTE magnitudes with the predicted REDMAG subsystem values was done to validate the REDMAG algorithms. For the purposes of this analysis, a group of stars observed simultaneously in the FOV of RXTE ST 1 was chosen and divided into two subgroups, one of the stars not expected to have NN-related identification problems and the other stars in which at least one star of the pair has a bright NN. These stars were identified in the *Tycho Catalogue* and independent *Tycho* positions and *V* magnitudes were obtained.

TRACKER POSITION PERFORMANCE COMPARED WITH *TYCHO*

Star-Pair Angular Separations:

Angular separations of star pairs were calculated both from the RXTE FOV coordinates and from the *Tycho* positions. For the stars with NN's brighter than approximately $V = 10.0$, the effects on the observed RXTE star by its near-neighbor were measured in a shift in position relative to another observed RXTE star in the FOV at the same time.

Figure 2 shows the effects of NN interference on the measured position of the centroid by plotting the deviation of the predicted pair separation from the measured separation (taken as measured minus predicted) as a function of NN angular separation ($\Delta\theta$) and the magnitude difference (Δm) of the primary and secondary NN stars. The horizontal axis represents the NN $\Delta\theta$ in arcseconds, while the vertical axis represents the component Δm (in magnitudes), and the contours are the measured $\Delta\theta_o$ minus the predicted $\Delta\theta_p$ in arcseconds. The horizontal axis is marked in one-pixel increments. The location of each data point used in the plot has been superimposed over the contours as an oval symbol. The region in the lower left-hand corner corresponds to stars with small NN separations and a bright companion star. Due to these characteristics, this region ($0 \leq \Delta m \leq 1$; $0 \leq \Delta\theta \leq 60$) is devoid of features because the attitude determination software rejected the stars seen by the star tracker for identification. The difference between the $\Delta\theta_o$ and $\Delta\theta_p$ separations is probably not bounded; the maxima and minima in Figure 2 probably indicate regions in which star identification often fails in the software. The 10-arcsecond or less contours correspond to the noise (standard deviation between the $\Delta\theta_o$ and $\Delta\theta_p$ values for the group of stars without interfering NN's). This number is in good agreement with the 6 arcsecond error (in each coordinate) found during calibration maneuvers early in the RXTE mission (Ref. 2).

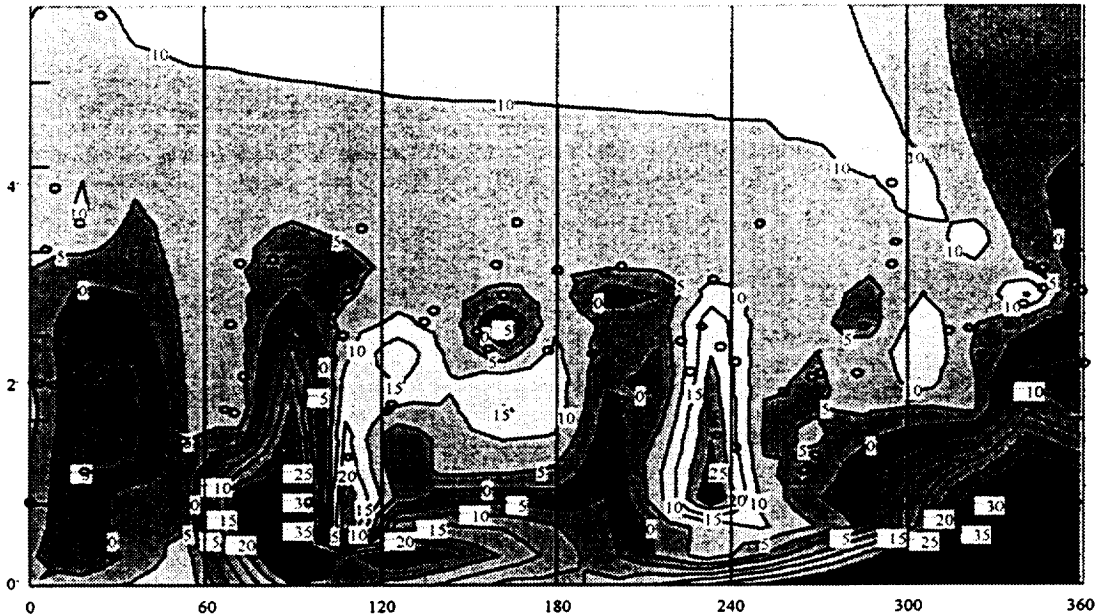


Figure 2 Near-Neighbor Effects on Measured Separations (Arcseconds)

CCDST MAGNITUDE MEASUREMENT COMPARED TO PREDICTION

Star-Pair Magnitude Differences:

All observed RXTE stars have V magnitudes obtained either from the *Tycho Catalogue*, the *Catalog of Red Magnitudes* (Ref. 3), or from the *Mermilliod UB V Catalogue* (Ref. 4). These magnitudes are not directly useful, as the sensitivity curves of the CCDSTs on RXTE are not close to that of the Johnson V passband (see Figure 3). However, these magnitudes together with available Johnson and Cousins red magnitudes from Reference 3 (R passband) could be used as input to the REDMAG magnitude prediction subsystem of the MMSCAT catalog generation software. REDMAG uses the sensitivity curve of the RXTE CCDSTs (an average of the curves for trackers 1 and 2) together with spectrophotometric scans of different stellar spectral types to calculate a color correction (CI) to the input astronomical magnitude in order to predict the instrumental RXTE m_s . See the Appendix and Ref. 5 for discussions of REDMAG algorithms. The residuals between measurement and prediction were investigated for the stars without an interfering near neighbor and found to be in accordance with results documented elsewhere (Ref. 6), and then separately for the subgroup where at least one star of the pair was expected to show the effects of NN interference.

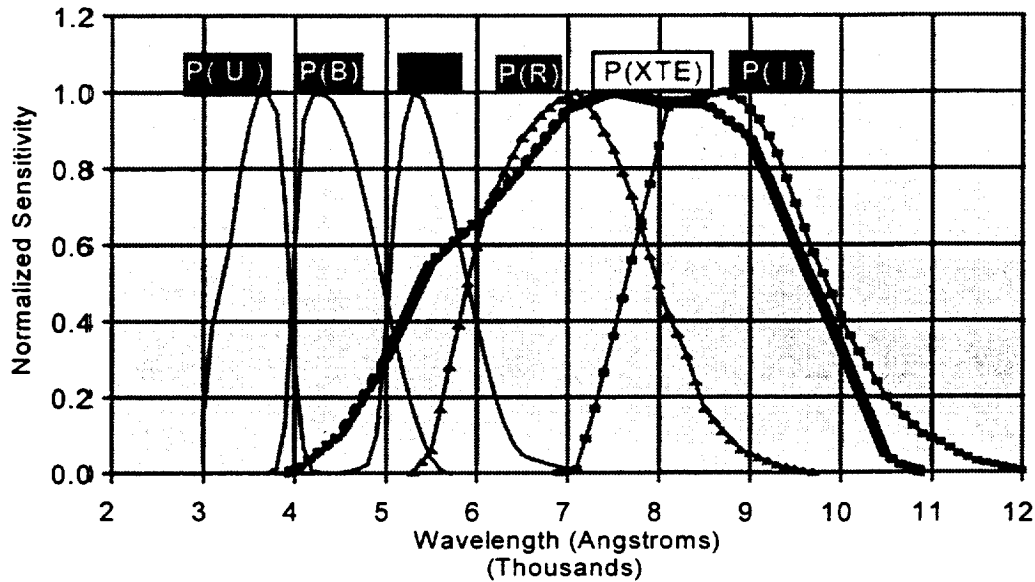


Figure 3 Johnson Standard UBVRI Passbands Compared to Ball Aerospace CT-601 Sensitivity Curve (Rossi XTE)

For the stars with interfering NN's, the magnitude residuals were then related to separations and magnitude differences obtained from various catalog sources, usually *Tycho* or the *Washington Catalog of Visual Double Stars 1994.0* (Ref. 7), with the qualifier that predicted sensor magnitudes for the primaries and secondaries were used to generate sensor passband magnitude differences for the pairs involved. Also, it was apparent that the observed sensor magnitudes from the defocused CCDST images can be modeled better by using the standard astronomical formula for a blended pair magnitude with the standard astronomical passband magnitudes and magnitude differences replaced by predicted sensor magnitudes and magnitude differences (compare Figures 4 and 5, see Eq. 1).

$$m(\text{blend}) = m(\text{primary}) - 2.5 \log_{10}(1 + 2.5119^{-\Delta m}) \quad (1)$$

Figure 4 shows the effects of NN interference on the measured CCDST magnitudes, expressed as the difference between the measured sensor magnitude and the unblended predicted magnitude. The horizontal and vertical axes are the same as in Figure 2, but the contours in Figure 4 represent the difference between the measured and predicted magnitudes of the stars. The magnitude difference on the vertical axis is the sensor passband magnitude difference, and the horizontal axis represents the separation in arcseconds between the primary and secondary components of the pair.

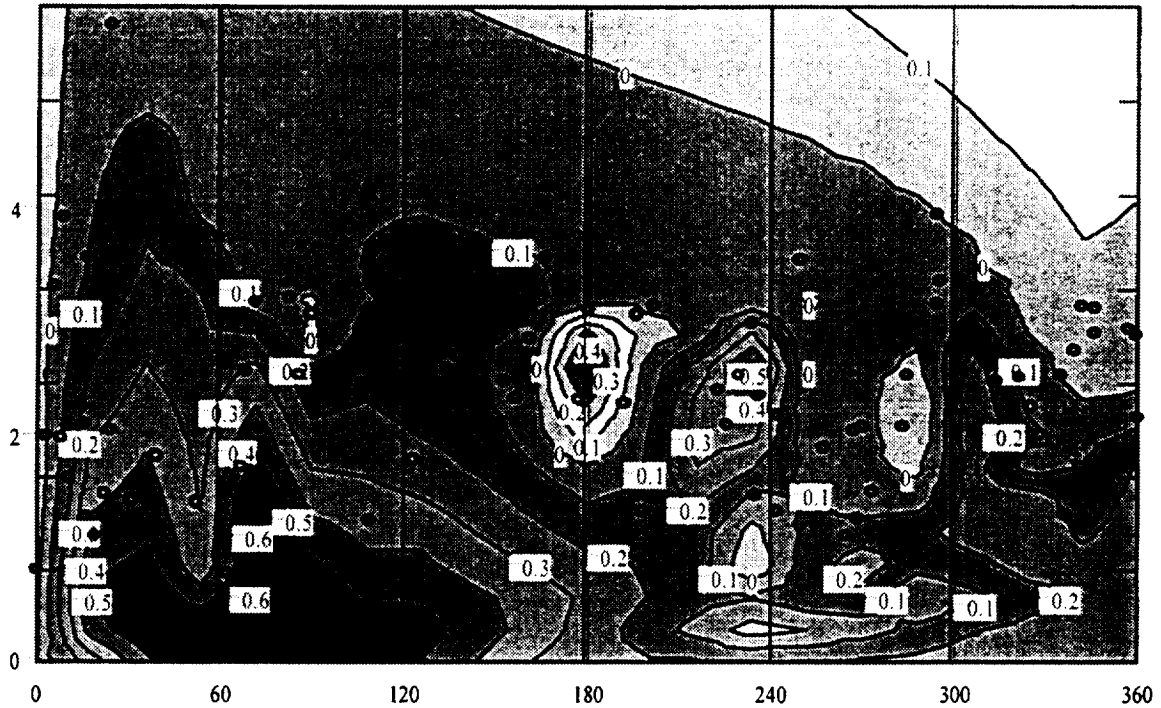


Figure 4 Near-Neighbor Effects on Measured Magnitude, Non-Blended Predicted Magnitudes

Figure 5 is the same plot, but using blended predicted magnitudes, where the blended magnitude is computed from the predicted primary magnitude and the sensor passband magnitude difference. Both figures show features near the CCDST pixel boundaries which may be associated with the algorithm used by the manufacturer to sum the incident flux and produce a measured sensor magnitude. Further analysis of this effect may require knowledge of the manufacturer's algorithm, which is not available at present. Figure 5 shows an improvement in the agreement of the predicted magnitudes with the measured magnitudes over the region in which a blended image is seen by the tracker, but the blended predicted values become too bright in the region in which the tracker begins to separate the images (4-5 pixels separation).

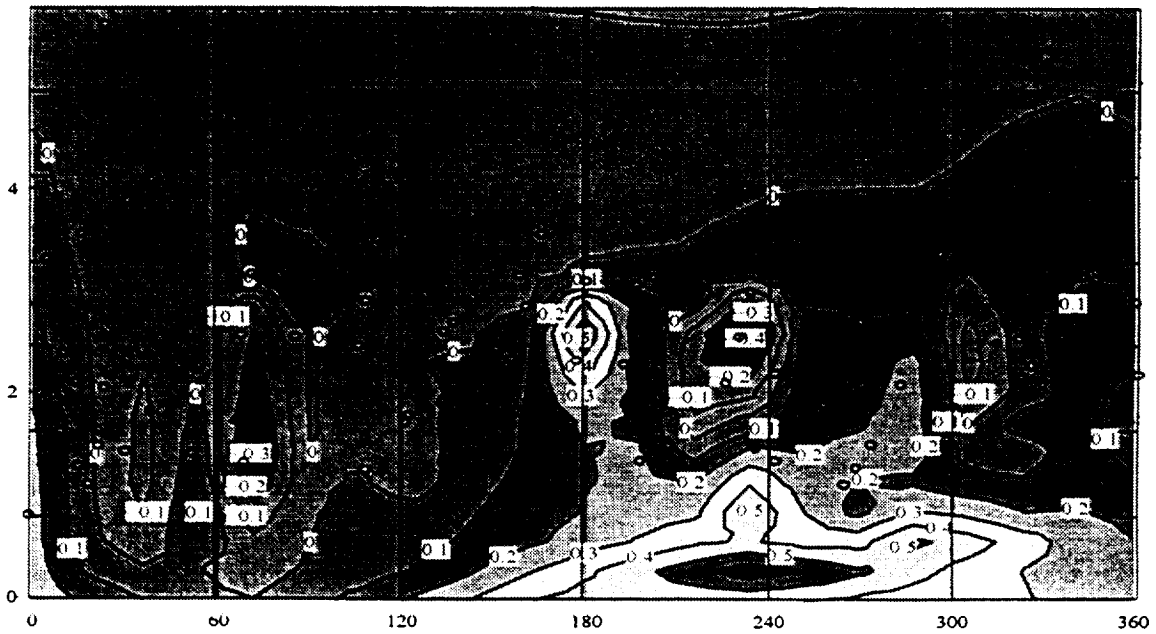


Figure 5 Near-Neighbor Effects on Measured Magnitude, Blended Predicted Magnitudes

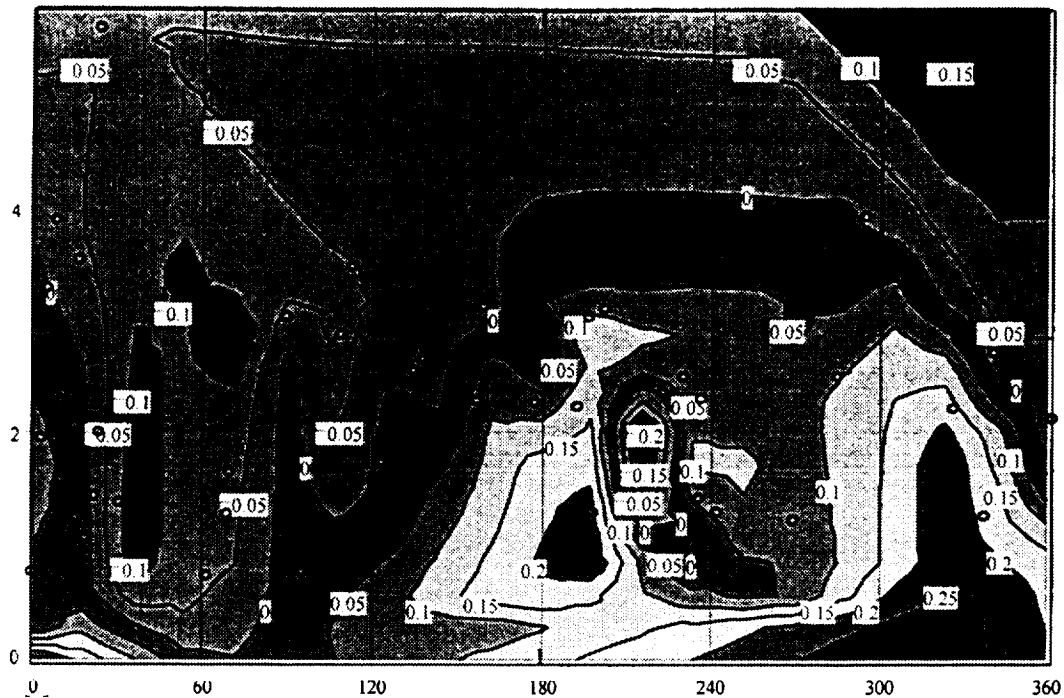


Figure 6 Near-Neighbor Effects on Measured Magnitude, Blended Predicted Magnitudes (Spectral Types O-F)

Since the CT-601 CCDST is known to be selectively more sensitive in red wavelengths, the stars plotted in Figures 4 and 5 were further separated into two groups, one composed of stars with spectral types between O and F, and one composed of stars with spectral types K, M, or redder. Figures 6 and 7 highlight the fact that the predicted magnitudes are not as accurate for the redder stars, as expected (Ref. 6). The region in Figure 7 corresponding to NN's brighter than two magnitudes fainter than the primary and closer than 4 pixels (240 arcseconds) is devoid of data points, which may indicate that the star identification software fails for red primary stars in this region.

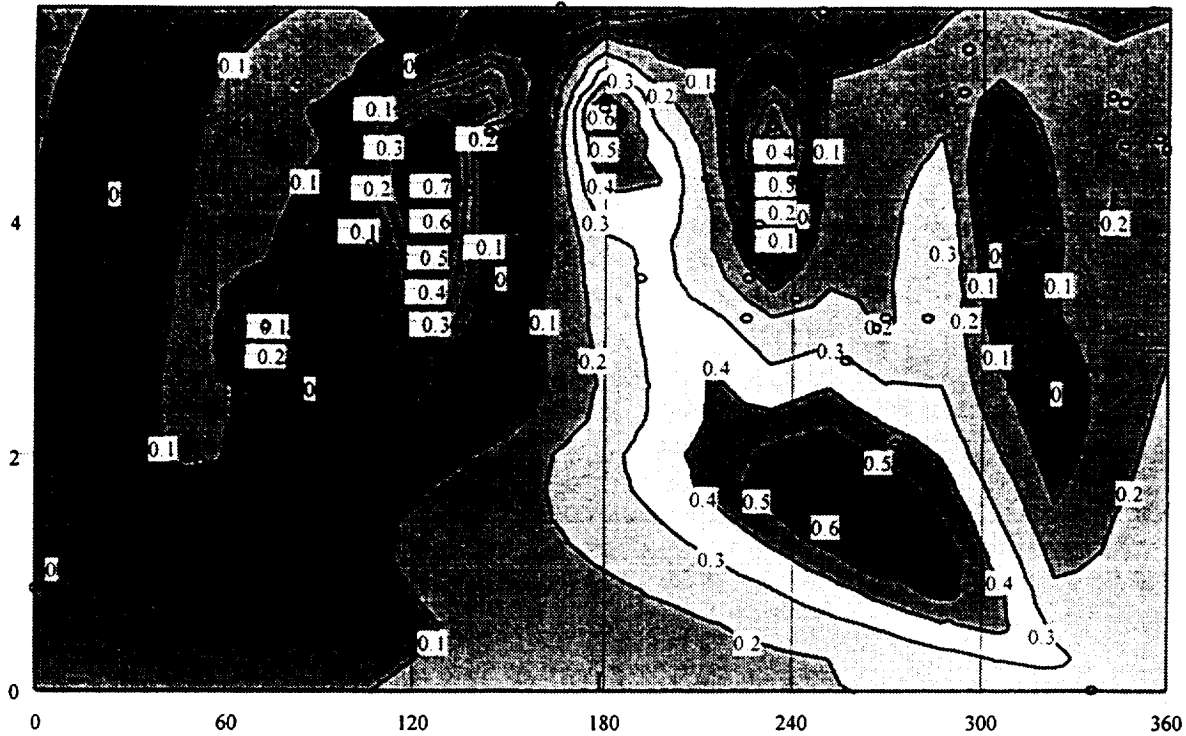


Figure 7 Near-Neighbor Effects on Measured Magnitude, Blended Predicted Magnitudes (Spectral Types K, M, and Redder)

DISCUSSION

The manufacturer of the CT-601 CCDST states that NN's separated by more than four pixels (240 arcseconds) from a measured star should have a greatly reduced effect on the position determination. This appears to be well borne out by the data. For example, replacement of primary component positions with center-of-light positions showed no significant improvement in the residuals in the region where blended magnitudes improved the magnitude residuals (less than four pixels NN separation). Calculated positions can deviate by tens of arcseconds from predicted values in cases of extreme interference, but most attitude determination software applies constraints to the identification process and properly setting them can eliminate many of the affected stars from an attitude solution. Also, there does seem to be a significant pixel edge-related effect on the measured positions, but at this point in the analysis it has not been examined closely (Figure 2).

The manufacturer also recommends that no star brighter than 4 magnitudes fainter than a potential candidate catalog star be located within 0.1 degree (6 pixels) of that candidate star in order to reduce the contamination of the image. Within this 0.1-degree region, it appears that stars 3 or more magnitudes fainter than the catalog star produce little or no observable interference (Figure 5). As the NN brightness

and position approaches the catalog star, the interference increases until the image measured by the star tracker deviates too much from the catalog prediction, whereupon most attitude software will reject the star. This situation can be improved by the use of blended sensor magnitudes for pairs separated by approximately 3 pixels (compare Figures 4 and 5), but the blended magnitudes are less accurate than unblended predictions at separations of approximately four or more pixels (Figure 5). The positive deviations in Figure 5 indicate that the blended predictions are brighter than what is observed, possibly indicating that the tracker no longer sees a blended image.

The recommendation from the manufacturer that stars with NN's violating the preceding constraints be excluded from a mission star catalog would probably be too harsh a restriction. Instead, alterations in the NN data fields of the input MC and in the REDMAG subsystem of the MMSCAT software could be made in order to produce better predictions for CCDST's. Catalog entries could be blended into single entries for stars with significantly interfering NN's, which would also eliminate a problem seen for stars with NN separations of around four pixels, in which the identification produced by the attitude software "flip-flops" between the two stars of the pair. A single, blended catalog entry would obviously eliminate the possibility of a "flip-flop" in the software and is probably a better prediction of what the CCDST will see for stars with interfering NN's.

ACKNOWLEDGMENT

The authors wish to acknowledge the contributions of the following personnel to this paper:

- Joseph A. Hashmall
- Joanne R. Myers
- Flight Dynamics Attitude Operations personnel, notably Jonathan S. Landis and Craig U. Woodruff

REFERENCES

- 1.) European Space Agency, *Hipparcos and Tycho Catalogues*, ESA SP-1200, 1997.
- 2.) Goddard Space Flight Center, Flight Dynamics Division, CSC 10032526, Rossi X-Ray Timing Explorer (RXTE) Postlaunch Report, D. Fink, W. Davis, et al. (CSC), June, 1996.
- 3.) Warren Jr., W., *Northern Hemisphere Catalog of Red Magnitudes*, 1994.
- 4.) Mermilliod, J.C., *Catalogue of Homogeneous Means in the UBV System*, Institut d'Astronomie, Universite de Lausanne, 1994.
- 5.) Goddard Space Flight Center, Flight Dynamics Division, CSC-27434-41, SKYMAP Requirements, Functional, and Mathematical Specifications, Volume 2, Revision 1, Instrumental Red Magnitude Prediction Subsystem, A.C. Miller, D. Brasoveanu, C. Sande, (CSC), D.A. Tracewell (NASA/GSFC), W.H. Warren Jr. (Raytheon STX), prepared by the Computer Sciences Corporation, June 1997, pp. 4.6-4 & 4.6-5.
- 6.) Goddard Space Flight Center, Flight Dynamics Division, 56830-04, SWAS Run Catalog Prelaunch Analysis, A.C. Miller, R. Nieman, prepared by the Computer Sciences Corporation, September, 1996.
- 7.) Worley, C.E. and G.G. Douglass, *Washington Catalog of Visual Double Stars 1994.0*, United States Naval Observatory, 1994.

APPENDIX

Instrumental Magnitude Prediction Algorithm

The instrumental red-magnitude prediction subsystem (REDMAG) in the MMSCAT software package computes the expected instrumental color index (CI_{SZ}) [sensor color correction] from a stellar magnitude (m_Z) observed through an astronomical passband (Z) and the spectral type (MK) both recorded in the *Master Star Catalog (MC)*, and the characteristics of the Z passband response curve (P_Z) and sensor passband (S) sensitivity curve (P_S). m_Z is corrected by CI_{SZ} to give the expected sensor magnitude ($m_S = m_Z + CI_{SZ}$). The CI_{SZ} algorithm follows from Reference 5:

$$CI_{SZ} = -25 \log_{10} \left\{ \frac{\langle\langle P_S \bullet N \otimes 10^{-0.4W(\lambda)A_V} \rangle\rangle \langle\langle P_Z \bullet N^{A_V} \rangle\rangle \langle\langle P_V \bullet N^* \rangle\rangle}{\langle\langle P_Z \bullet N \otimes 10^{-0.4W(\lambda)A_V} \rangle\rangle \langle\langle P_S \bullet N^* \rangle\rangle \langle\langle P_V \bullet N^{A_V} \rangle\rangle} \right\}$$

where each set of double brackets $\langle\langle \bullet \rangle\rangle$ gives the energy flux of the stellar spectrum (N) intercepted by the response curve (P). The Morgan-Keenan-Johnson (MK) spectral type gives access to the proper spectrophotometric spectrum in the REDMAG scan file. Each scan is normalized to 1.0 at the effective wavelength (λ_{eff}^V) of the visual passband (V) and each response curve is normalized to 1.0 at its maximum value. All N 's and P 's are functions of wavelength (λ) and their product function is defined as

$$\langle\langle P \bullet N \rangle\rangle = \int_0^{\infty} P(\lambda)N(\lambda)d\lambda \approx \sum_{i=1}^{np} P(\lambda_i)N(\lambda_i)\delta\lambda_i$$

where

np = the total number of data points in the summation

Specific variables and functions are defined as

CI_{SZ} = notation for the (S - Z) sensor color

Z = V (typically); the preferred order of use for the RXTE mission is red (R) first, then V when R is not available, then photovisual (pv), followed by infrared (I), blue (B), photographic (ptg), or ultraviolet (U) as available

P_V = response curve of the V passband

P_S = sensitivity curve of the sensor (S)

P_Z = response curve of an observed standard astronomical passband (Z)

N = normalized stellar spectrophotometric scan

A_V = interstellar absorption index in the V passband is computed using the difference between the observed color $(B-V)_{obs}$ and intrinsic [standard] color $(B-V)_{int}$; the MK spectral type of the star in the MC gives access to the REDMAG standard colors file.

$W(\lambda)$ = Whitford interstellar reddening function normalized to λ_{eff}^V

$N \otimes 10^{-0.4W(\lambda)A_V}$ = stellar spectral scan reddened by interstellar absorption

N^{A0V} = spectral scan of an $A0V$ reference type

($*$) = typically $A0V$, $G0V$, $K0V$ or other reference selected for the mission sensor; frequently different from the standard $A0V$ reference used for astronomical passbands ($UBVRI$)

$N^{(*)}$ = normalized spectral scan for the mission sensor reference type ($*$)

In general, the contribution from each of three ratios in the CI_{SZ} expression above is given by

$$\Delta CI_{SZ}(\text{ratio}) = -2.5 \log_{10}(\text{ratio value})$$

Once the value of ($*$) has been selected for the mission, the contribution of the last ratio is a constant, unchanged for all stars and all observed astronomical passbands. [Examples: ($*$) = $A0V$ and $\Delta CI_{SZ}(\text{last}) =$ zero for the RXTE; ($*$) = $G0V$ and $\Delta CI_{SZ}(\text{last}) = 0.455$ magnitude for the SWAS.] Similarly, $\Delta CI_{SZ}(\text{middle})$ is unchanged for all stars but does change with the observed astronomical passband used in each computation. $\Delta CI_{SZ}(\text{first})$ changes with each star and the observed passband (Z) used. Due to the non-flat stellar spectrum of the typical star, it is clear that the closer λ_{eff}^Z , effective bandwidth ($\Delta \lambda_{eff}^Z$), and shape of P_Z is to P_S the closer $\Delta CI_{SZ}(\text{first})$ comes to zero and the less critical the uncertainty in the computation. See Figure 8 for the product functions $P_S \bullet N$ and $P_V \bullet N$ for RXTE.

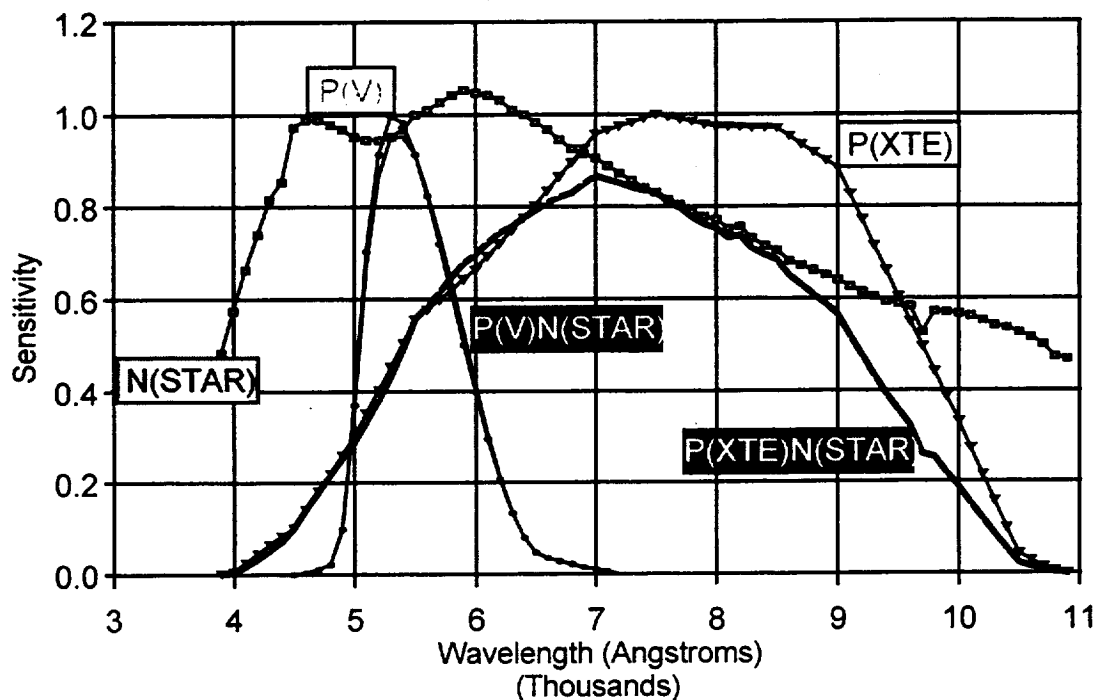


FIGURE 8 TYPICAL STAR MEASURED IN V & XTE (BALL CT-601) BANDS

Usually $Z = V$ and P_Z becomes P_V since there are many more accurate, observed m_V 's in the MC than any other magnitude. The first equation above reduces to the following:

$$CI_{SV} = -25 \log_{10} \left\{ \frac{\left\langle \left\langle P_S \cdot N \otimes 10^{-0.4W(\lambda)A_v} \right\rangle \right\rangle}{\left\langle \left\langle P_V \cdot N \otimes 10^{-0.4W(\lambda)A_v} \right\rangle \right\rangle} \frac{\left\langle \left\langle P_V \cdot N^* \right\rangle \right\rangle}{\left\langle \left\langle P_S \cdot N^* \right\rangle \right\rangle} \right\}$$

The $CI_{SV} = m_S - m_V$ is the sensor color correction supplied by the vendor which includes the effect of the reference spectral type ($*$) selected for the mission. At the selected reference, $CI_{SV} = 0$ ($m_S = m_V$). Note that at the selected reference, when $Z \neq V$, in general $CI_{SZ} \neq 0$ ($m_S \neq m_Z$).